ELSEVIER

Ceramics International 25 (1999) 681–687

CERAMICS INTERNATIONAL

# Sintering behavior of $Al_2TiO_5$ base ceramics and their thermal properties

M. Nagano [a], S. Nagashima [b,*], H. Maeda [a], A. Kato [c]

[a] *Department of Chemistry and Biochemistry, Graduate School of Engineering, Kyushu University, 6-10-1, Hakozaki, Higashi-ku, Fukuoka 812-8581, Japan*

[b] *Tohwa Institute for Science, Tohwa University, 1-1-1, Chikushigaoka, Minami-ku, Fukuoka 815-8510, Japan*

[c] *Department of Applied Chemistry, Kumamoto Institute of Technology, Ikeda 4-22-1, Kumamoto 860-0082, Japan*

Received 9 April 1998; received in revised form 5 May 1998; accepted 24 July 1998

**Abstract**

Sintering behavior of $Al_2TiO_5$ without and with various additives and the thermal properties of the sintered material—thermal expansion and decomposition—were investigated. The precursors of $Al_2TiO_5$ powders were prepared by homogeneous precipitation and coprecipitation. Sintering of pure $Al_2TiO_5$ gave a fine grained-structure at 1300°C, but resulted in large-grained and cracked microstructures at 1400 and 1500°C. Addition of $ZrO_2$ or BaO gave fine-grained microstructures with a small increase in thermal expansion. Addition of $ZrO_2$, BaO or $ZrSiO_4$, especially $ZrSiO_4$, was effective in suppressing the thermal decomposition of $Al_2TiO_5$ at 1100°C. 

*Keywords:* A. Sintering; C. Thermal expansion; D. $Al_2TiO_5$; Additives

## 1. Introduction

Aluminum titanate ($Al_2TiO_5$) is characterized as a low thermal expansion material having a melting point as high as 1860°C. However, its low expansion is due to a prominent thermal expansion anisotropy which tends to cause cracks in the sintered bodies, making it difficult to obtain a high-density [1]. In addition, $Al_2TiO_5$ decomposes into $\alpha$-$Al_2O_3$ and $TiO_2$ (rutile) in the temperature range 900–1280°C. The mechanical strength of $Al_2TiO_5$ ceramics increases as the grain size decreases [2]. To suppress the decomposition of $Al_2TiO_5$ and to prepare the fine-grained ceramics, many investigators have examined the effect of various additives such as MgO, $SiO_2$ or $ZrO_2$ [3–8]. Yano et al. [9,10] investigated thermal and mechanical properties of $Al_2TiO_5$–mullite composites.

In the present paper, the sinterability of fine powder of $Al_2O_3$–$TiO_2$ hydrate prepared by homogeneous precipitation and the effects of addition of low-thermal-expansion glass, barium salts, $ZrO_2$ and $ZrSiO_4$ on the sintering behavior of the $Al_2O_3$–$TiO_2$ system were investigated.

## 2. Experimental procedure

### 2.1. Preparation of powder and sintering

#### 2.1.1. Homogeneous precipitation method

Titanium oxysulfate ($TiOSO_4$), aluminum sulfate ($Al_2(SO_4)_3$) and urea ($(NH_2)_2CO$) were dissolved in distilled water. The solution was heated at 90°C and was stirred by a motor-driven stirrer (1700 r.p.m.) during synthesis until the pH of the solution reached 6.0. The product was centrifugally collected, rinsed and dried in vacuum at 70°C. The powder was then calcined in air at 800 to 1300°C for 1 h. After compaction into discs, the green compacts were sintered in air at temperatures in the 1300 to 1500°C range for 4 h.

#### 2.1.2. Coprecipitation method

$Al_2TiO_5$ precursor was obtained by a coprecipitation of mixing the sulfate ($[Al_2(SO_4)_3]=[TiOSO_4]=0.05$ mol dm$^{-3}$, 250 cm$^3$) and $NH_4OH$ (2 N, 100 cm$^3$) solutions. The precipitate was rinsed and dried in a vaccum at 70°C and was calcined in air at 1000°C for 1 h. This calcined powder and the additives were mixed in ethanol. For $Al_2TiO_5$–$ZrSiO_4$ composite, the calcined and $ZrSiO_4$ powders ($ZrSiO_4$; commercial powder irregular

* Corresponding author.

0272-8842/99/$ - see front matter 
PII: S0272-8842(98)00083-2

shape particles below 4 μm in diameters) were mixed in the same way. After drying, the mixed powder was isostatically pressed to discs of approximately 10 mm diameter. The green compact was sintered in air at 1300 to 1400°C for 4 h.

### 2.2. Analysis

The powders were analyzed by thermoanalysis (TG-DTA). The crystal phases of the samples were identified by X-ray diffraction (XRD) using $CuK_\alpha$ radiation. The amount of the $Al_2TiO_5$ phase in the calcined powders and sintered products was calculated from the calibration curves which were made by using the X-ray diffraction intensities of (113) of $\alpha$-$Al_2O_3$, (110) of $TiO_2$ (rutile) and (110) of $Al_2TiO_5$. The specimens for thermal decomposition were heated in an electric furnace at 1100°C for the prescribed time, and were quenched rapidly to room temperature.

The densities of the green and sintered compacts were obtained using a cathetometer and the Archimedes method, respectively. The theoretical density of $Al_2TiO_5$ and $ZrSiO_4$ used were 3.702 and 4.70 g cm$^{-3}$, respectively. The morphology of as-synthesized powder and of fracture surfaces of sintered bodies was observed under a scanning electron microscope (SEM). The sintered bodies were analyzed with an energy-dispersion X-ray microanalyzer (EDX) for aluminum and titanium.

### 2.3. Measurement of thermal expansion

The variations of volume of the sintered bodies with the temperature were measured with a thermal mechanical analysis apparatus (TMA). Specimens for measurement were pressed to rods of 5 mm in diameter and 10–20 mm in length, and sintered for 4 h at prescribed temperatures. The $\alpha$-$Al_2O_3$ (the thermal expansion coefficient: $8.0\times10^{-6}$ K$^{-1}$) was used as reference specimen. Heating or cooling rates were 5°C min$^{-1}$. The thermal expansion coefficient was calculated from the measurements in the 100 to 1000°C range.

## 3. Results and discussion

### 3.1. Homogeneous precipitates

The precipitation conditions were [urea] = 10.0 mol dm$^{-3}$ and [$TiOSO_4$] = [$Al_2(SO_4)_3$] = 0.01 mol dm$^{-3}$

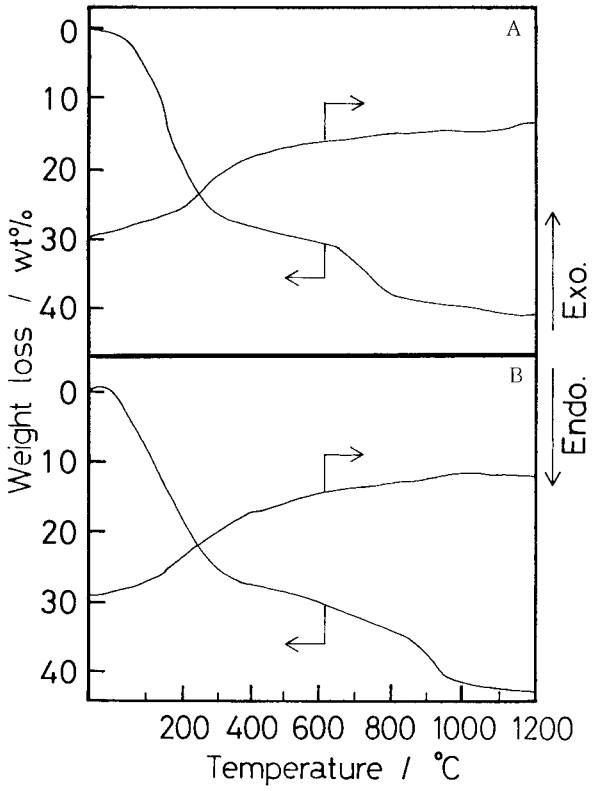


Fig. 2. TG-DTA curves of the homogeneous precipitates measured at heating rate 10°C min$^{-1}$ in the flow of air. A and B for samples are the same as in Fig. 1. DTA; full scale is ±25 μV.

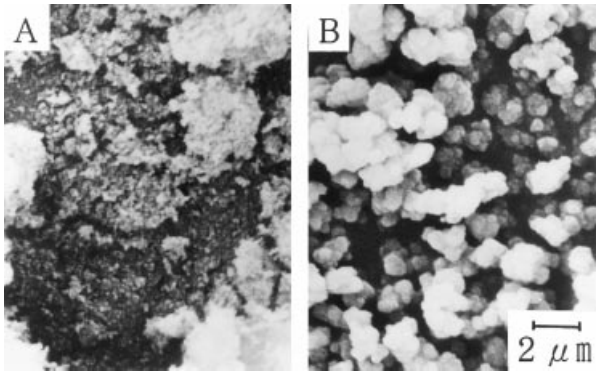


Fig. 1. SEM photograghs of powders prepared by homogeneous precipitation method. Precipitation conditions: [$Al_2(SO_4)_3$] = [$TiOSO_4$] = 0.01 mol dm$^{-3}$ (A), 0.025 mol dm$^{-3}$ (B), [$(NH_2)_2CO$] = 10.0 mol dm$^{-3}$; temperature = 90°C.

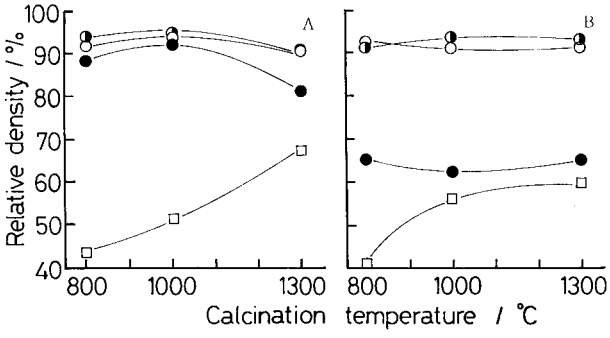


Fig. 3. Effects of calcination and sintering temperature on densification. Green body: □. Sintering temperature: ●, 1300°C; ◑, 1400°C; ○, 1500°C. Sintering time: 4 h. Calcination time: 1 h. A and B for samples are the same as in Fig. 1.

Table 1
Crystalline phase in calcined powders

| Calcination temperature (°C) | X-ray analysis | | |
|---|---|---|---|
| | Homogeneous precipitate | | Coprecipitate |
| | (A) | (B) | |
| As-prepared | Amorphous | Amorphous | Amorphous |
| 800 | A | A | A |
| 900 | A, AT | – | A |
| 1000 | AT, A | R, C, A | AT, R, C, A |
| 1100 | R, C, AT | – | R, C |
| 1200 | – | – | R, C |
| 1250 | R, C | R, C | – |
| 1300 | AT, R | R, C, AT | R, C, AT |

Key: A = $TiO_2$ (anatase), R = $TiO_2$ (rutile), C = α-$Al_2O_3$ (corundum), AT = $Al_2TiO_5$. Calcination time: 1 h.

(A) and 0.025 mol $dm^{-3}$ (B). The precipitates are shown in Fig. 1. $TiO_2$ hydrate particles precipitate first and $Al_2O_3$ hydrate particles follow with the rise of solution pH due to hydrolysis of urea. The small size of particles (A) is probably due to precipitation taking place rapidly at low salt concentration. On the other hand, precipitates (B) form slowly under high salt concentration, and the particle growth occurs by aggregation of small particles into the larger particles. TG-DTA curves are shown in Fig. 2. Dehydration of both powders occurred below ca. 400°C. The decomposition of the sulfate group occurred above 600°C in specimen (A) and above 800°C in specimen (B). The decomposition temperature is believed to change depending on particle size. Crystalline phases found in calcined powders are summarized in Table 1. The precipitates were amorphous; both

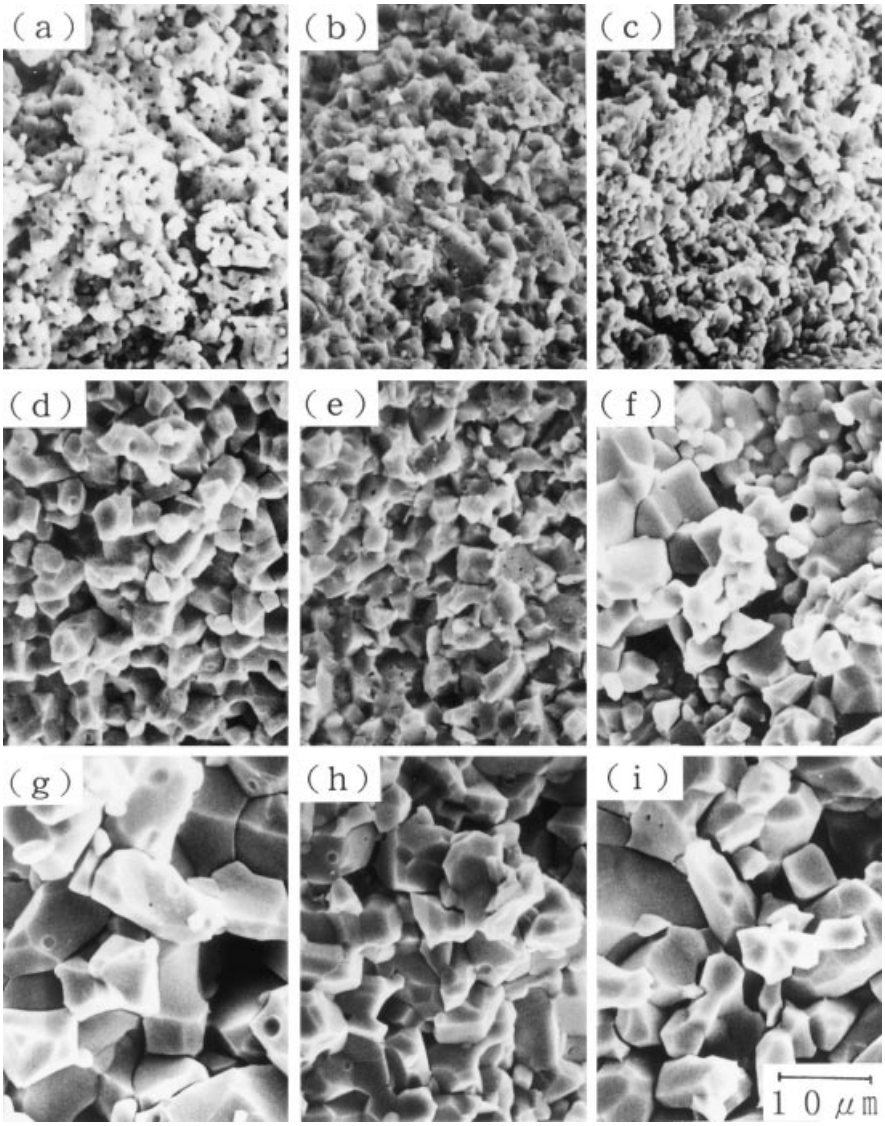


Fig. 4. SEM photograghs of fracture surfaces of specimen (A) sintered. Calcination and sintering temperatures: (a) 800°C, 1300°C; (b) 1000°C, 1300°C; (c) 1300°C, 1300°C; (d) 800°C, 1400°C; (e) 1000°C, 1400°C; (f) 1300°C, 1400°C; (g) 800°C, 1500°C; (h) 1000°C, 1500°C; (i) 1300°C, 1500°C.

products calcined at 800°C contained an anatase phase. $Al_2TiO_5$ phase was found at 1000°C in powder (A) and at 1300°C in powder (B). The equilibrium temperature for $\alpha$-$Al_2O_3 + TiO_2$ (rutile) $\rightleftarrows Al_2TiO_5$ is 1285°C. The formation of $Al_2TiO_5$ at 1000°C in powder (A) seems to be due to the thermodynamically unstable state of both reactants, amorphous $Al_2O_3$ and $TiO_2$ (anatase).

The effects of calcination and sintering temperatures on densification are shown in Fig. 3. $Al_2TiO_5$ was the main crystal phases of all sintered bodies. In the case of specimen (A), relative densities of sintered bodies were around 90%. Fracture surfaces of specimen (A) are shown in Fig. 4. At sintering temperatures of 1400 and 1500°C, a marked grain growth and many cracks were observed. Specimen calcined at 1000°C and sintered at 1300°C had 92% of theoretical density and a microstructure with about 2 μm in grain diameters [Fig. 4(b)]. The high sintered density and the fine microstructure are probably due to an $Al_2TiO_5$ phase produced in the powder calcined at 1000°C which would serve as nucleus to promote reactions in sintering.

In the case of specimen (B), relative densities of sintered bodies at 1300°C were below 70% as shown in Fig. 3. At a sintering temperature of 1500°C, the grains grow, and there were many cracks. By sintering at 1400°C, the powder calcined at 1000°C gave a sintered body having relatively small grain size with 94% of theoretical density.

### 3.2. Coprecipitates and effect of additives

#### 3.2.1. Properties of $Al_2TiO_5$ precursor prepared by coprecipitation method

SEM photograghs of precipitates and crystal phases of calcined powders are shown in Fig. 5 and Table 1, respectively. The coprecipitates were aggregates consisting of primary particles of about 50 nm in diameter. $Al_2TiO_5$ is formed by calcination at 1000°C as shown in Table 1. The formation of $Al_2TiO_5$ may be explained as well as in the powder (A) prepared in homogeneous precipitation method. From this result, calcination was done at 1000°C in the following.

Fig. 6(a) shows a SEM photograph of the fracture surface of sintered body at 1300°C. $Al_2TiO_5$ sintered body consisted of crystal grains of about 10 μm, and large cracks existed in the body. Small grains of 2–3 μm in diameter were observed in the large grains.

#### 3.2.2. Effects of additives on microstructures of sintered bodies

Ten weight percent of glass powders were added to $Al_2TiO_5$ in order to accelerate the sintering and control the microstructure. By adding $Na_2O$–$B_2O_3$–$SiO_2$, CaO–$Al_2O_3$–$SiO_2$ or ZnO–$B_2O_3$–$SiO_2$ glass powders, the grains of the sintered bodies grew and the density of sintered body or $Al_2TiO_5$ formation ratio decreased in several combinations of sintering temperature and additives. By adding PbO–$B_2O_3$–$SiO_2$ glass powder, the formation of $Al_2TiO_5$ was inhibited and the density of sintered body became low. Needle-like grains were observed as shown in Fig. 6(b) which were found to be $TiO_2$ (rutile) by EDX and XRD analyses. It is thought that excess $TiO_2$ crystallized because the $Al_2O_3$ component dissolved in the glass.

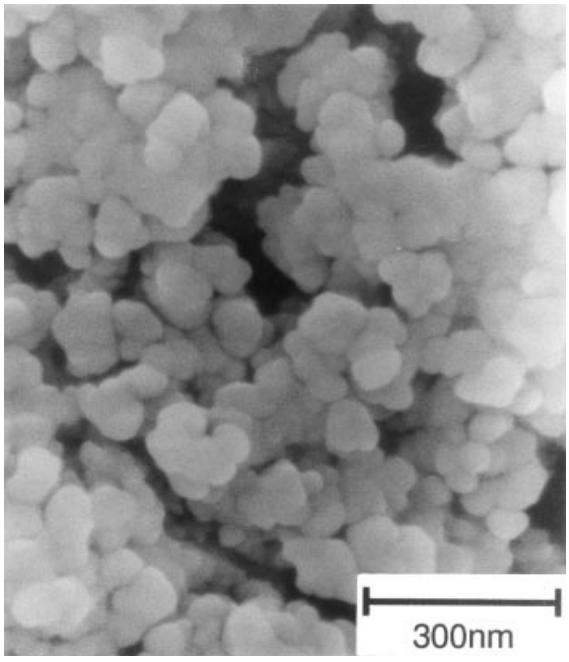


Fig. 5. SEM photograghs of an $Al_2TiO_5$ precursor prepared by coprecipitation. Precipitation conditions: $[Al_2(SO_4)_3] = [TiOSO_4] = 0.05$ mol dm$^{-3}$ (250 cm$^3$), $[NH_4OH] = 2.0$ mol dm$^{-3}$ (100 cm$^3$).

Sintered bodies with a fine microstructure were obtained by addition of PbO–BaO–$SiO_2$ or CaO–BaO–$SiO_2$ glass powder [Fig. 6(c)]. The depression of grain growth by both BaO containing additives was confirmed with 10 mol% addition of $Ba(NO_3)_2$, $BaCl_2$ or $BaCO_3$. Regardless of the kind of barium salts, the structure of the sintered bodies became fine-grained with increasing concentration of barium salts [Fig. 6(d)] and there were no cracks in grain boundaries of the sintered body. Crystalline phase and relative densities of sintered bodies are summarized in Table 2. BaO reacted with the $Al_2O_3$ component to form $BaAl_2O_4$ in the sintered body. The addition of $ZrO_2$ was also very effective for suppression of grain growth [Fig. 6(e)] in a similar manner as in past studies [2,3], and, in this case, $ZrTiO_4$ formed in the sintered body. It is thought that $BaAl_2O_4$ phase or $ZrTiO_4$ phase formed in the sintered body existed at grain boundaries and depressed grain growth. Cracks might not occur easily in grain boundaries because the stress due to cooling after sintering was small due to fine grain sizes.

The thermal expansion curves are shown in Fig. 7. The thermal expansion ratio of specimens without

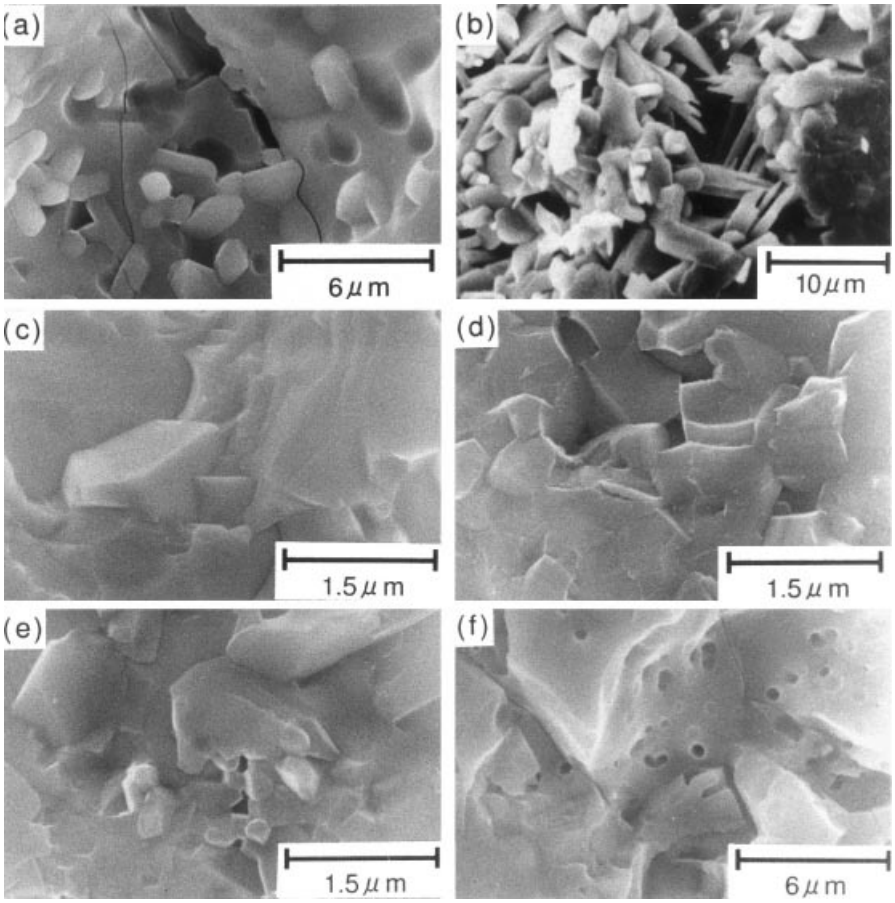


Fig. 6. SEM photograghs of the fracture surfaces of $Al_2TiO_5$ sintered bodies. (a) No additive, (b) 10 wt% PbO–$B_2O_3$–$SiO_2$, (c) 10 wt% CaO–BaO–$SiO_2$, (d) 10 mol% $Ba(NO_3)_2$, (e) 5 mol% $ZrO_2$, (f) 80 mol% $Al_2TiO_5$–20 mol% $ZrSiO_4$. Sintering conditions: 4 h at 1300°C (a–e) and at 1400°C (f). Green and sintered densities (%): (a) 52, 92; (b) 56, 82; (c) 55, 85; (d) 56, 93; (e) 56, 94; (f) 57, 93.

Table 2
Analysis results of sintered bodies with additives

| Additive | Sintering temperature (°C) | Relative density | X-ray analysis |
|---|---|---|---|
| None | 1300 | 92 | AT, R, C |
| | 1350 | 91 | AT, R, C |
| | 1400 | 91 | AT |
| 10 mol% $Ba(NO_3)_2$ | 1300 | 93 | AT, R, C, BA |
| | 1350 | 89 | AT, BA |
| | 1400 | 90 | AT, R, C, BA |
| 10 mol% $BaCO_3$ | 1300 | 96 | AT, R, C, BA |
| | 1350 | 94 | AT, R, C, BA |
| | 1400 | 92 | AT, R, C, BA |
| 10 mol% $BaCl_2$ | 1300 | 92 | AT, R, C, BA |
| | 1350 | 91 | AT, BA |
| | 1400 | 91 | AT, R, C, BA |
| 5 mol% $ZrO_2$ | 1300 | 94 | AT, R, C, ZT |
| | 1350 | 88 | AT, R, ZT |
| | 1400 | 88 | AT, R, ZT |

Key: AT = $Al_2TiO_5$, R = $TiO_2$ (rutile), C = α-$Al_2O_3$ (corundum), BA = $BaAl_2O_4$, ZT = $ZrTiO_4$.

additives became small with increasing sintering temperature [Fig. 7(a)]. A microcracking phenomenon takes place during cooling from the sintering temperature, due to the unusually strong anisotropy in thermal expansion of the orthorhombic β-$Al_2TiO_5$ crystallites ($\alpha_a = 11.8\times10^{-6}$ $K^{-1}$, $\alpha_b = 19.4\times10^{-6}$ $K^{-1}$, $\alpha_c = 2.6\times10^{-6}$ $K^{-1}$). The thermal expansion of the specimen sintered at higher temperature was small because of the existence of more cracks due to grain growth. The sample without additives showed large hysteresis in thermal expansion. The thermal expansion coefficient of the sintered body with BaO or $ZrO_2$ additives, obtained by sintering at 1300°C, was a little larger and the hysteresis became smaller than in the absence of additives. This may be due to the near absence of cracks in these doped sintered bodies.

### 3.2.3. *$Al_2TiO_5$–$ZrSiO_4$ composite sintered body*

Properties of the $Al_2TiO_5$–$ZrSiO_4$ composite sintered bodies were investigated for $Al_2TiO_5$ contents from 0 to 100 mol%. $ZrSiO_4$ has a high strength and a low thermal expansion.

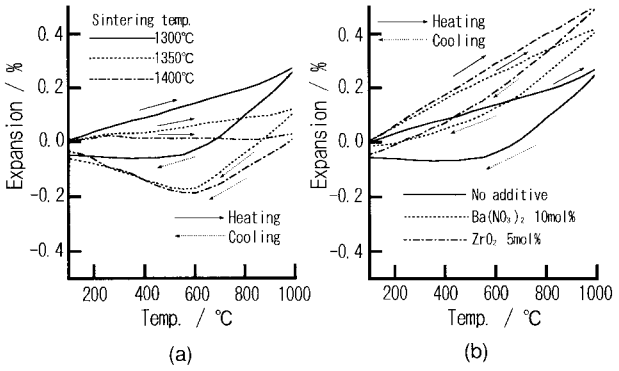


Fig. 7. Thermal expansion curves of $Al_2TiO_5$ ceramics. Heating and cooling rate = 5°C $min^{-1}$. (a) Effect of sintering temperature on $Al_2TiO_5$ without additives sintered for 4 h. (b) Effect of additives on $Al_2TiO_5$ sintered for 4 h at 1300°C.

Effects of $Al_2TiO_5$ content and sintering temperature on densification are shown in Fig. 8. Only in the case of sintering at 1400°C and $Al_2TiO_5$ contents above 60 mol%, the $ZrTiO_4$ phase formed. In the case of small $Al_2TiO_5$ content, the density following sintering at 1300–1400°C is low. This may be due to the low sinterability of $ZrSiO_4$ which is normally sintered at 1500–1600°C [11]. The grain size decreased with increasing $ZrSiO_4$ content. The fracture surface of the 80 mol% $Al_2TiO_5$–20 mol% $ZrSiO_4$ specimen sintered at 1400°C is shown in Fig. 6(f). The microstructure was finer than that of specimen without additives sintered at 1300°C [Fig. 6(a)].

The relationship between the thermal expansion coefficient over 100–1000°C and $Al_2TiO_5$ content is shown in Fig. 9. Below 50 mol% $Al_2TiO_5$, the thermal

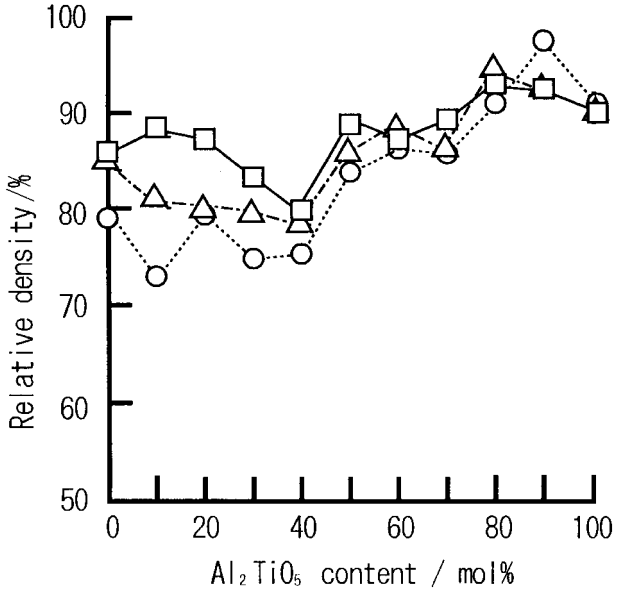


Fig. 8. Effect of composition on bulk density of $Al_2TiO_5$–$ZrSiO_4$ composites sintered for 4 h. Sintering temperature: ○, 1300°C; △, 1350°C; □, 1400°C.

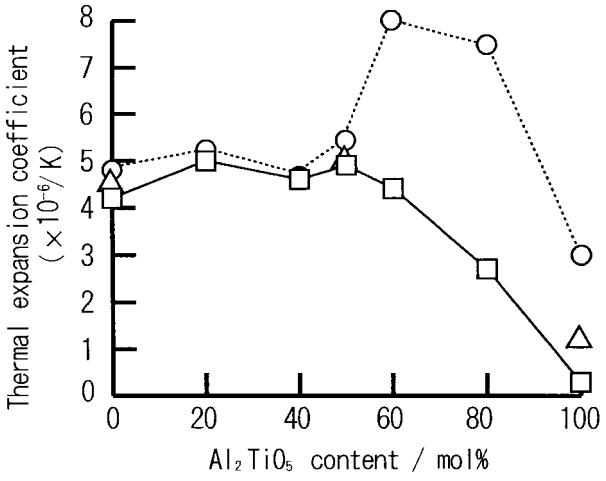


Fig. 9. Thermal expansion coefficients of $Al_2TiO_5$–$ZrSiO_4$ composites sintered for 4 h. Sintering temperature: ○, 1300°C; △, 1350°C; □, 1400°C.

expansion coefficient did not change with $Al_2TiO_5$ content and sintering temperature. On the other hand, above 50 mol% $Al_2TiO_5$, the thermal expansion coefficient decreased with increase of $Al_2TiO_5$ content in sintering at 1400°C. It became a maximum value at 60 mol% $Al_2TiO_5$ and then decreased with increase of $Al_2TiO_5$ content in sintering at 1300°C.

In the case of low $Al_2TiO_5$ content, the microstructure did not affect the thermal expansion coefficient because the main phase $ZrSiO_4$ shows essentially low thermal expansion. At large $Al_2TiO_5$ content, $ZrSiO_4$ grains are dispersed in the $Al_2TiO_5$ matrix. When sintering at 1300°C, $ZrSiO_4$ depressed grain growth of $Al_2TiO_5$ which is considered to be responsible for the large thermal expansion coefficients of 60 and 80 mol% $Al_2TiO_5$ composites. By sintering at 1400°C, grain growth was more pronounced, and cracks were produced at the grain boundaries. The 80 mol% $Al_2TiO_5$–20 mol% $ZrSiO_4$ composites had a fine microstructure with 93% of theoretical density and low thermal expansion, $2.7\times10^{-6}$ $K^{-1}$.

### 3.2.4. Thermal decomposition of $Al_2TiO_5$

$Al_2TiO_5$ ceramics decomposed into α-$Al_2O_3$ and $TiO_2$ (rutile) below 1280°C. It was reported that the decomposition rate was fastest between 1100 and 1180°C [12–15]. In the present study, the sintered specimens were heated at 1100°C. The thermal decomposition curves are shown in Fig. 10. The specimen sintered at 1300°C without additives decomposed about 75% in 8 h, but in $Ba(NO_3)_2$, $ZrO_2$ or $ZrSiO_4$ added sinters, decomposition was depressed markedly. For the specimen with 80 mol% $Al_2TiO_5$–20 mol% $ZrSiO_4$ was sintered at 1400°C, the decomposition was not detected in 8 h. Kato et al. [12] reported that the decomposition process is nucleation and growth-controlled and that nucleation at the grain boundaries of sintered samples is

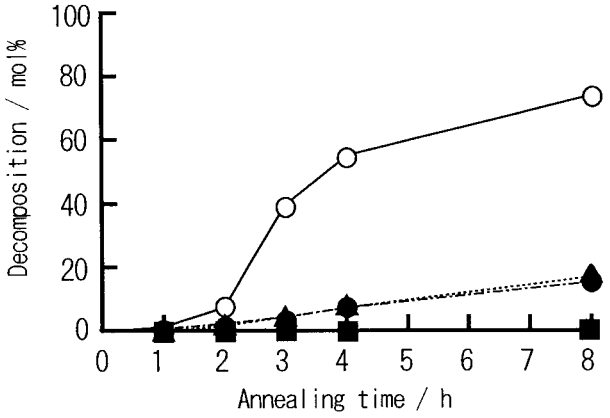


Fig. 10. Effect of isothermal (1100°C) annealing time on the decomposition of $Al_2TiO_5$. Key: ○, no additive, sintered at 1300°C; ●, 10 mol% $Ba(NO_3)$ addition, sintered at 1300°C; ▲, 5 mol% $ZrO_2$ addition, sintered at 1300°C; ■, 80 mol% $Al_2TiO_5$–20 mol% $ZrSiO_4$, sintered at 1400°C.

favored by densification. The decomposition in these doped sintered bodies would be depressed by the decrease of cracks at grain boundaries and the stabilization of grain surfaces by covering them with $BaAl_2O_4$, $ZrTiO_4$ or $ZrSiO_4$.

## 4. Conclusions

1. $Al_2TiO_5$ powder prepared by a homogeneous precipitation method was sintered at 1300 to 1500°C. The precipitation conditions were $[urea]=10.0\ mol\,dm^{-3}$, $[TiOSO_4]=[Al_2(SO_4)_3]=0.01\ mol\,dm^{-3}$ (A) and $0.025\ mol\,dm^{-3}$ (B) and temperature = 90°C. Formation of the $Al_2TiO_5$ phase was confirmed by heating at 1000°C for powder (A) and at 1300°C for powder (B).

By sintering powder (A) at 1400 and 1500°C, grains grew markedly and cracks were observed at grain boundaries. Specimens sintered at 1300°C using powder calcined at 1000°C had 92% TD and a fine microstructure with about 2 μm grains. The high sintered density and fine microstructure are probably due to $Al_2TiO_5$ phase produced in the calcination at 1000°C which served as nuclei to promote reaction in sintering.

Powder (B) gave sintered densities above 90% TD at 1400 and 1500°C while below 70% TD at 1300°C. Sintering at 1500°C resulted in large grains and many cracks in the sintered bodies. Sintering at 1400°C of powder previously calcined at 1000°C gave a sintered body having fine grain sizes with 94% TD.

2. An $Al_2TiO_5$ powder prepared by coprecipitation was sintered and the effect of additives on the microstructure of sintered body was investigated. The addition of $ZrO_2$ or BaO was very effective for suppressing grain growth, and led to dense sintered bodies having a fine microstructure consisting of about 1 μm grains. $BaAl_2O_4$ or $ZrTiO_4$ phase formed during sintering depressed grain growth. With BaO or $ZrO_2$ addition, the thermal expansion coefficient of the sintered bodies became a little larger, but the hysteresis became small. Composite sintered at 1400°C with 80 mol% $Al_2TiO_5$–20 mol% $ZrSiO_4$ has a fine microstructure and relatively low thermal expansion. BaO, $ZrO_2$ and $ZrSiO_4$ depressed thermal decomposition of $Al_2TiO_5$ at 1100°C.

## Acknowledgements

This research was supported in part by a grant from a Grand-in-Aid for Scientific Research from the Japanese Ministry of Education, Science and Culture (no. 06650968). The energy-dispersion X-ray microanalyzer at the Center of Advanced Instrumental Analysis, Kyushu University was used for elemental analysis.

## References

[1] K. Hamano, Aluminum titanate ceramic, Taikabutu 27 (1975) 520–527.
[2] Y. Ohya, K. Hamano, Z. Nakagawa, Microstructure and mechanical strength of aluminum titanate ceramics prepared from synthesized powders, Yogyo-kyokai-shi 91 (1983) 289–297.
[3] Y. Ohya, K. Hamano, Z. Nakagawa, Effects of some additives on microstructure and bending strength of aluminum titanate ceramics, Yogyo-kyokai-shi 94 (1986) 665–670.
[4] K. Hamano, Z. Nakagawa, K. Sawano, Y. Hasegawa, Effects of additives on several properties of aluminum titanate ceramics, J. Chem. Soc. Jpn. 1981 (1981) 1647–1655.
[5] D.S. Perera, Reaction-sintered aluminium titanate, J. Mater. Sci. Lett. 8 (1989) 1057–1059.
[6] F.J. Parker, R.W. Rice, Correlation between grain size and thermal expansion for aluminum titanate materials, J. Am. Ceram. Soc. 72 (1989) 2364–2366.
[7] M. Kajiwara, Sintering and properties of stabilized aluminium titanate, Br. Ceram. Trans. J. 86 (1987) 77–80.
[8] H. Wholfromm, J.S. Moya, P. Pena, Effect of $ZiSiO_4$ and MgO additions on reaction sintering and properties of $Al_2TiO_5$-based materials, J. Mater. Sci. 25 (1990) 3753–3764.
[9] T. Yano, N. Nagai, M. Kiyohara, K. Saito, N. Ootsuka, Thermal and mechanical properties of aluminumtitanate–mullite composites: 1. Effects of composition, Yogyo-kyokai-shi 94 (1986) 970–976.
[10] H. Morishima, Z. Kato, K. Uematsu, K. Saito, T. Yano, N. Ootsuka, Development of aluminum titanate–mullite composite having high thermal shock resistance, J. Am. Ceram. Soc. 69 (1986) C226–C227.
[11] T. Itoh, Zircon ceramics prepared from hydrous zirconia and amorphous silica, J. Mater. Sci. Lett. 13 (1994) 1661–1663.
[12] E. Kato, K. Daimon, J. Takahashi, Decomposition temperature of β-$Al_2TiO_5$, J. Am. Ceram. Soc. 63 (1980) 355–356.
[13] E. Kato, Y. Kobayashi, K. Daimon, Factors affecting decomposition rate of $Al_2TiO_5$, Yogyo-kyokai-shi 86 (1987) 626–631.
[14] T. Kameyama, T. Yamaguchi, Kinetic studies on the eutectoid decomposition of $Al_2TiO_5$, Yogyo-kyokai-shi 84 (1976) 589–593.
[15] H.A.J. Thomas, R. Stevens, Aluminium titanate—a literature review: 1. Engineering properties and thermal stability, Br. Ceram. Trans. J. 88 (1989) 184–190.